



**FUPRE Journal**

of

**Scientific and Industrial Research**








ISSN: 2579-1184(Print)

ISSN: 2578-1129 (Online)

<http://fupre.edu.ng/journal>

**Application of Response Surface Methodology and Artificial Neural Network Analytical approach in modelling Shock Resistance of Pipeline Weldments**

**MABIAKU, T.A.**<sup>1</sup> , **ACHEBO, J. I.**<sup>1</sup> , **OBAHIAGBON, K. O.**<sup>2</sup> , **OZIGAGUN, A.**<sup>1</sup> ,  
**UWOGHIREN, F. O.**<sup>1,\*</sup> 

<sup>1</sup>Department of Production Engineering, University of Benin, Benin City

<sup>2</sup>Department of Chemical Engineering, University of Benin, Benin City

**ABSTRACT**

**ARTICLE INFO**

Received: 23/09/2023

Accepted: 23/12/2023

**Keywords**

Artificial Neural Network, Response surface Methodology, Shock Resistance, Structural Integrity

Heat transfer, given its various applications, has long been the focus of researchers and engineers. However, Shock Resistance also takes on a pivotal role in transporting an array of fluids and gases across various industrial domains. This study bridges this discrepancy by scrutinizing the after-effects of a specific non-elastic factor, namely shock resistance, on pipeline weldments and its interaction with elastic properties. This investigation unveils the intricate interrelation, underscoring the necessity of encompassing non-elastic facets to ensure the dependability of pipeline weldments across various operational contexts. Cutting-edge techniques, such as machine learning algorithms and finite element simulations, are harnessed to accurately predict and optimize these non-elastic factors (Shock Resistance), thereby enhancing the overall strength and structural integrity of pipeline weldments. The experimental setup adheres to the central composite design, meticulously constructed using design expert software (version 13.0). The response surface methodology analysis yields optimal outcomes, suggesting a current of 160.000 amps, voltage of 21.280 volts, and gas flow rate of 14.667 liters per minute. These parameters collectively yield a welded joint with a shock resistance value of 0.729, achieving a desirability value of 0.918. Additionally, the artificial neural network model is employed to predict output parameters and compared against the RSM methodology. The findings underscore the pivotal role of optimizing non-elastic performance factors in pipeline weldments. By accurately anticipating and controlling temperature, engineers and professionals within the pipeline sector can design weldments capable of enduring harsh conditions, curbing the risk of failures, and significantly prolonging pipeline operational lifespans.

\*Corresponding author, e-mail: [timothy.mabiaku@gmail.com](mailto:timothy.mabiaku@gmail.com)

DIO

©Scientific Information, Documentation and Publishing Office at FUPRE Journal

## 1. INTRODUCTION

The construction and operation of pipelines for the transportation of various fluids, such as oil, gas, and water, constitute a critical aspect of modern industrial infrastructure (Seyyedattar et al., 2020). Ensuring the strength and structural integrity of pipeline weldments is of paramount importance to prevent potential failures that can result in severe environmental, economic, and safety consequences (Biezma et al., 2020). While substantial attention has been given to optimizing factors like tensile strength and fatigue resistance in pipeline weldments, there exists a noticeable research gap when it comes to the prediction and enhancement of shock resistance – a crucial yet understudied aspect that directly influences the ability of pipelines to withstand sudden impact loads and dynamic stresses. Historically, research efforts have predominantly concentrated on optimizing the elastic performance characteristics of pipeline weldments, such as yield strength and Young's modulus. However, there exists a notable gap in the literature concerning the prediction and enhancement of non-elastic properties, particularly shock resistance. The term 'shock resistance' describes a material's capacity to endure abrupt and powerful impacts without undergoing deformation or failure. This property is particularly relevant for pipeline weldments that are subjected to dynamic loading events, such as seismic activities, machinery vibrations, and impact forces (Prabowo et al., 2021). Shock resistance, defined as the capacity of a material or structure to absorb

energy during impact, plays a pivotal role in maintaining the reliability of pipeline systems (Shojaei et al., 2021). The integrity of pipeline weldments in the face of shock events, such as accidental impacts or seismic disturbances, is critical to preventing catastrophic failures that can lead to leakage, rupture, and subsequent environmental pollution or loss of life (Nwankwo, 2021). Given the diverse and often harsh operating conditions that pipelines are subjected to, from underground installations to offshore environments, optimizing shock resistance becomes a priority to ensure their robust performance and long-term durability (Rubino et al., 2020). The optimization and prediction of shock resistance to enhance the strength and structural integrity of pipeline weldments is a pivotal area of research within the realm of material science and engineering (Tabatabaeian et al., 2022). Pipelines are indispensable components of various industries, facilitating the efficient transportation of fluids and gases over extensive distances. The ability of these pipelines to withstand dynamic and sudden loading conditions, commonly referred to as shock loading, is of paramount importance to ensure the safety, reliability, and longevity of the entire infrastructure (Elahibakhsh, 2023).

Optimizing shock resistance necessitates a comprehensive understanding of the underlying mechanisms that contribute to a material's ability to absorb and dissipate shock energy (Wang et al., 2022). Factors such as microstructural characteristics, material composition, heat treatment

---

\*Corresponding author, e-mail: [timothy.mabiaku@gmail.com](mailto:timothy.mabiaku@gmail.com)

DIO

©Scientific Information, Documentation and Publishing Office at FUPRE Journal

processes, and welding techniques play a crucial role in influencing shock resistance. Therefore, a holistic approach that encompasses material science, metallurgy, mechanical engineering, and computational modelling is imperative to tackle this multifaceted challenge (Callister Jr., 2018). While research within the realm of pipeline engineering has traditionally focused on static mechanical properties, the importance of dynamic response characteristics, particularly shock resistance, is increasingly being recognized. Recent advancements in science of materials, computational modelling, and experimental techniques have paved the way for a more comprehensive understanding of shock behaviour in pipeline weldments. Investigating the interplay between microstructure, material properties, and shock resistance is crucial for designing weldments that can withstand sudden and unpredictable impact loads (Quazi et al., 2021). It is noteworthy that a comprehensive approach to optimizing shock resistance involves not only the selection of appropriate materials but also the meticulous design of weld geometries, joint configurations, and fabrication techniques (Laska and Szkodo, 2020). This multifaceted optimization process requires a thorough understanding of the mechanical behaviour of materials under shock loading conditions, as well as the utilization of advanced simulation tools and experimental validation methods (Sharma et al., 2022). Recent advancements in machine learning and artificial intelligence have also contributed to the prediction and optimization of shock resistance. These

technologies facilitate the analysis of complex data sets and the identification of hidden patterns that impact shock resistance (Baduge et al., 2022). By harnessing machine learning algorithms, researchers can develop predictive models that guide the optimization of welding parameters, material combinations, and structural configurations to bolster shock resistance (Dogra, 2018). In the quest to augment the shock resistance of pipeline weldments, this study aims to bridge the existing research gap by comprehensively exploring the dynamic response of various pipeline materials and weldment configurations to impact loading (Li, 2021). The utilization of finite element simulations, coupled with empirical testing, will allow for the accurate prediction of shock resistance and the identification of critical design parameters (Makarian and Santhanam, 2020).

In this present paper, the authors used Response Surface Methodology (RSM) and Artificial Neural Network (ANN) to model and analyse the intricate relationship between current, voltage and gas flow rate with respect to shock resistance of pipeline weldments. Though, other algorithms have previously been employed, however, RSM and ANN have not been comparatively combined in modelling shock resistance of pipeline weldments. By addressing this research gap, engineers and scientists can pave the way for the development of pipeline weldments that can withstand unexpected impact loads and contribute to the overall sustainability of pipeline systems.

## 2. METHODOLOGY

### 2.1 Process Parameters

The process the factors evaluated in this research study are the welding voltage, current, and gas flow rate in correspondence with the welding pool temperature. This study combined two 60 x 40 x 10 mm mild steel plates using twenty experimental runs totaling the current, voltage, and gas flow rate. A Brinell hardness test unit is used to perform the Brinell hardness test. In this experiment, a tungsten carbide sphere of a specified diameter (D) undergoes the application of a predetermined force (F), which is maintained for a predetermined duration (T) before being subsequently released. The metal specimen in the test undergoes a permanent deformation, leaving an impression created by a spherical indenter. Obtaining the indentation diameter (d) involves averaging measurements taken at two or more different locations inside the indentation. The loading system for the Brinell Hardness Testing Machine is made up of weights, levers, a plunger, and a hydraulic dashpot. The test substance is stored on the movable anvil. The spherical ball indenter hit the material using the lever and exerted a preset force that was displayed on the screen.

### 2.2 Design of Experiment

A scientific method for planning and carrying out an experiment that will demonstrate a cause-and-effect link between variables is known as the design of an experiment. It can also be a rigorous strategy

to changing the process inputs and examining the outcomes that result so that the cause-and-effect relationship between them and the random variability of the process can be measured with the fewest possible runs. Scientific research must include experimentation, which can be developed with the aid of computer programs like design expert and Minitab. Data is collected using an experimental methodology to ensure proper polynomial approximation. There are various experimental design kinds, such as full factorial, Latin hyper cube, central composite circumscribed, and central composite face centred.

The central composite design (CCD) was chosen, and the design expert software was utilized to build the experimental matrix. The CCD employs the mathematical procedure indicated in equation (1).

$$N = 2^n + 2n + k \quad (1)$$

Where N = Total number of experiments, n = number of input parameters.

The same program utilized for the model generation of all the responses is the design expert software. The core composite design of experiment was chosen based on the quantity of input parameters.

### 2.3 Materials and Experimental Set-up

Thermocouples were attached to gas tungsten arc welding (GTAW) technique. It occurred at an operating current range of 150 to 200 A, on a 200 x 200 x 20 mm<sup>3</sup> a low-carbon steel block and a DCEN (Direct Current Electrode Negative) with a 4 mm

arc gap was employed as a shielding gas. Temperatures between 1500 and 1800 °C were recorded. The thermocouples were W5 tungsten thermocouples. The thermocouple has good resistance to high temperatures and an overall diameter of 1.2 mm, including the sleeving and tungsten wires. The samples contained the thermocouples at a depth of 4 mm, a diameter of 1.4 mm, and an angle of 20°. The thermocouple attached to the sample of weld.

#### 2.4 Method of Data Collection

Twenty test runs for the center composite design matrix were produced utilizing the design expert software. The parameters for the input and output, as well as the results mentioned for the data acquired from the weld sample, are all part of the experimental matrix. The formula  $2n + 2n + k$ , where  $k$  is the quantity of center points,  $2n$  is the quantity of axial points, and  $2n$  is the quantity of factorial points, provides the number of input parameters, which determines the size of the data matrix. Using RSM (Response Surface Methodology) and ANN (Artificial Neural Network), the data were examined.

#### 2.5 Response Surface Methodology

Engineers often utilize the Response Surface Methodology (RSM) to find the circumstances under which it best supports the desired operation. In essence, they look for values of the input parameters for the procedure that yield the best results. The optimal value determined by the input parameters of the process could either be a minimum or a maximum. RSM is one of the

optimization methodologies that is now used extensively to describe how the welding process functions and to determine the appropriate response. To achieve optimal results, RSM encompasses a range of mathematical and statistical techniques designed to predict and model the desired outcome. Numerous input factors have an impact on this result.

#### 2.6 Artificial Neural Network

A distributed, massively parallel computer called a neural network has a built-in propensity to store experimental data and make it usable for applications. As a data mining tool, it is employed to find undiscovered patterns in datasets. It resembles the brain in two respects. Within the network, learning takes place, and synaptic weights—the intensities of internal neuron connections—are used to store the information. The appropriate  $w$  is applied to the  $R$  input of a simple neuron. The bias added to the weighted inputs serves as the input to the transfer function  $f$ . Any differentiable transfer function  $f$  can generate the neurons' output. The transfer function  $\text{logsig}$  of a log-sigmoid is often used in multilayer networks. The function  $\text{logsig}$  generates outputs between 0 and 1 as the neuron's net input changes from a negative value to a positive infinity. Using a different strategy in multilayer networks using the tan-sigmoid transfer function. Sigmoid output neurons are commonly used to handle problems involving pattern recognition, whereas linear output neurons are typically used to address problems involving function fitting. The artificial

neural network is a data mining tool that makes use of the neuronal communication method that has been programmed into software and the theory of the human brain. It is a prediction tool that examines data through the processes of training, learning, validating, and testing.

### 3. RESULTS

#### 3.1 Modelling and Optimization using RSM

In this research, an effort is made to use response surface methodology (RSM) to create a second order mathematical relationship between a few input parameters, such as current (I), voltage (V), and gas flow rate (GFR), along with one response variable, shock resistance. Maximizing shock resistance was the optimization model's main goal.

The ultimate goal of the optimization procedure was to identify the current (Amp), voltage (Volt), and gas flow rate (l/min) input variables with the highest possible shock resistance.

In order to provide experimental findings required for the optimization method;

- i. For the statistical design of the experiment (DOE), the central composite design technique (CCD) was utilized. The development and optimization processes were carried out using a statistical program. For this specific situation, it was determined to employ Design Expert 7.01.
- ii. A second step involved creating an experimental design matrix with 20 experimental runs and eight (8) factorial points (2n), six (6) axial points (2n), and six (6) center points (k)

In order to ensure that the quadratic model was suitable for assessing the experimental findings, the sequential model sum of squares for the % dilution response was calculated, as shown in Table 1.

**Table 1:** Sequential model sum of square for shock resistance

Source	Sum of Squares	df	Mean Square	F-value	p-value	
Mean vs Total	9.83	1	9.83			
Linear vs Mean	0.2568	3	0.0856	2.38	0.1083	
2FI vs Linear	0.2756	3	0.0919	3.97	0.0327	
<b>Quadratic vs 2FI</b>	<b>0.2854</b>	<b>3</b>	<b>0.0951</b>	<b>61.92</b>	<b>&lt; 0.0001</b>	<b>Suggested</b>
Cubic vs Quadratic	0.0142	4	0.0035	18.22	0.0017	Aliased
Residual	0.0012	6	0.0002			
Total	10.66	20	0.5331			

The sequential model sum of squares table illustrates how the model fit becomes better as more addition of terms. Considering the

estimated sequential model sum of squares, the highest order polynomial that has significant additional terms and a non-



aliased model were chosen as the best match. The cubic polynomial was found to be aliased from the results of Table I, hence it cannot be used to fit the final model. Additionally, it was suggested that the quadratic and 2FI model suited the data the best, which supported the adoption of the quadratic polynomial in this research.

The lack of fit test was performed for each response to determine how the quadratic model describes the basic variation in the experimental data. Prediction cannot be made using a model with a considerable lack of fit. Table 2 displays the findings of the calculated lack of fit test for shock resistance.

**Table 2:** Lack of fit test for shock resistance

Source	Sum of Squares	df	Mean Square	F-value	p-value	
Linear	0.5764	11	0.0524	1.89	0.2492	
2FI	0.3007	8	0.0376	2.47	0.1628	
Quadratic	0.0154	5	0.0031	<b>0.1640</b>	<b>0.9924</b>	<b>Suggested</b>
Cubic	0.0012	1	0.0012	0.0341	0.9667	Aliased
Pure Error	0.0000	5	0.0000			

The model statistics based on the model sources that were derived for the response to

the shock resistance are displayed in Table 3.

**Table 3:** Model summary statistics for shock resistance

Source	Std. Dev.	R <sup>2</sup>	Adjusted R <sup>2</sup>	Predicted R <sup>2</sup>	PRESS	
Linear	0.1898	0.3082	0.1785	-0.1296	0.9411	
2FI	0.1521	0.6391	0.4725	0.1513	0.7071	
<b>Quadratic</b>	<b>0.0392</b>	<b>0.9816</b>	<b>0.9650</b>	<b>0.8600</b>	<b>0.1166</b>	<b>Suggested</b>
Cubic	0.0140	0.9986	0.9956	0.6908	0.2576	Aliased

Each entire model's r-squared, standard deviation, predicted r-squared, adjusted r-squared and predicted error sum of square (PRESS) statistics are displayed in the summary statistics of model fit. The ideal criteria for identifying the optimal model source are a low standard deviation, R-Squared close to one, and a relatively low

PRESS. The quadratic polynomial model was chosen for this investigation since, according to the results of Table III, it was indicated while the cubic polynomial model was aliased. Table IV shows the goodness of fit statistics to verify the quadratic model's suitability based on its capacity to maximize shock resistance.

**Table 4:** GOF statistics for shock resistance

<b>Std. Dev.</b>	0.0392	<b>R<sup>2</sup></b>	0.9816
<b>Mean</b>	0.7010	<b>Adjusted R<sup>2</sup></b>	0.9650
<b>C.V. %</b>	5.59	<b>Predicted R<sup>2</sup></b>	0.8600
		<b>Adeq Precision</b>	23.6150

It is thought that there is a reasonable agreement when the difference between the Predicted R<sup>2</sup> of 0.8600 and the Adjusted R<sup>2</sup> of 0.9650 is less than 0.2, indicating reasonable agreement. Adeq Precision, which measures the signal-to-noise ratio, should ideally be at least 4. With a ratio of 23.615, it suggests a strong signal. This model can effectively guide design decisions within the specified area. A comparison between the projected values and the actual values was done in order to find values or groupings of values that the model would

not have been able to detect readily. This comparison is shown in Fig. 1a, with a special emphasis on shock resistance. A Cook's distance plot was produced for various responses in the experimental data to look for probable outliers. Cook's distance estimates how the removal of a certain point can affect the regression. In order to rule out outliers, points with extremely high distance values relative to the rest should be given more attention. Fig. 1b shows the Cook's distance plot for shock resistance (SR).

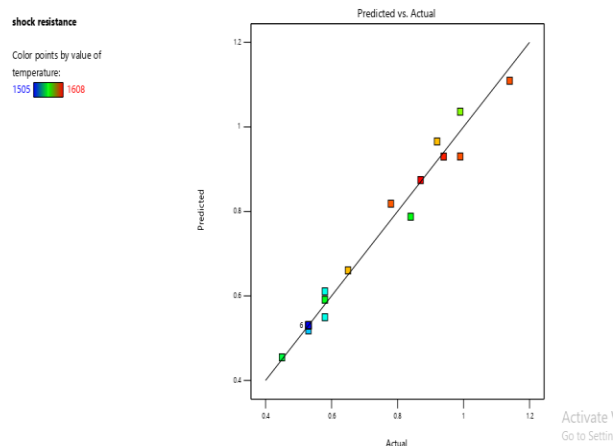


**Figure 1a:** Plot of Predicted Vs Actual for SR for SR.

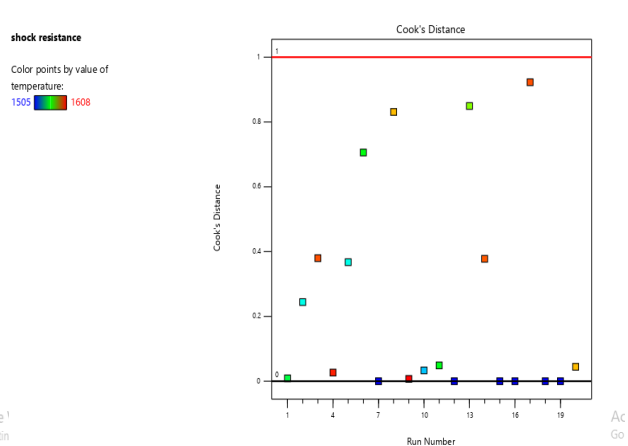


**Figure 1b:** Generated cook's distance for SR.

The graph in Fig. 1a shows how the dots are closely grouped around the fitted line. This shows that the model is successful in correctly predicting the bulk of the data

points. The Cook's distance plot, on the other hand, in Fig. 1b, its lower bound is 0.00 and its upper bound is 1.00. Outliers are considered experimental values that are



outside the expected range and require further examination. The results of Fig. 1a and 1b implies that the estimated residuals follow a distribution that is roughly normal. This is a good sign because it shows that the constructed model's accuracy and propensity

for prediction are sufficient. Fig. 1c represents 3D surface plots to analyze the effects of voltage and current on shock resistance while Fig. 1d surface plots were created to explore the effects of shock resistance on gas flow rate and current.

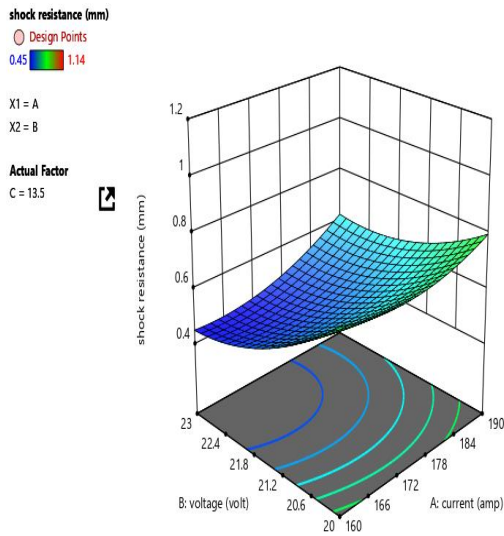


**Figure 1c :** Effect of current and voltage on SR on SR.

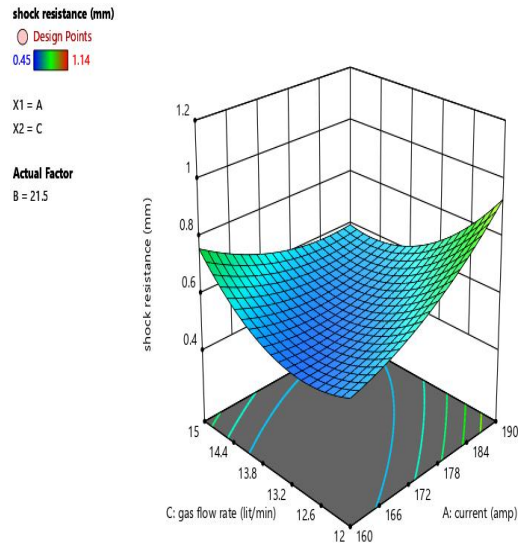


**Figure 1d:** Effect of current and flow rate on SR.

The 3D surface plots in Fig. 1e were designed to investigate the temperature impacts of voltage and gas flow rate. The

contour plots of the temperature response variable versus the ideal voltage and gas flow rate are shown in Fig. 1f.

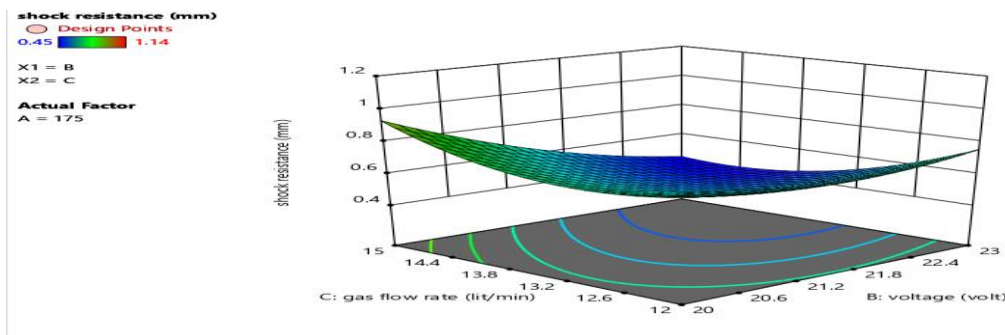


**Figure 1e:** Effect of voltage and gas flow rate on SR

**Figure 1f:** Predicting SR using contour plot

Table 5 displays the optimal outcomes of the numerical optimization.

**Table 5:** Optimal outcomes

S/N	Voltage	Gas flow rate	Shock Resistance	Remark	
<b>1</b>	<b>160.000</b>	<b>21.280</b>	<b>14.667</b>	<b>0.729</b>	<b>Selected</b>
2	160.000	21.286	14.676	0.730	
3	160.000	21.268	14.662	0.730	
4	160.000	21.303	14.690	0.730	
5	160.001	21.259	14.650	0.729	

### 3.2 Modelling of the Shock Resistance using Artificial Neural Network (ANN)

The examination also held significant value in establishing the precise mathematical link between the response (shock resistance) and the current, voltage, and gas flow rate are examples of input variables. In the pursuit of attaining an optimal network structure that provides the highest precision in comprehending the input-output data correlation, two pivotal aspects were taken into account. The initial aspect encompassed the selection of the most accurate training algorithm or learning rule. Secondly, the determination of the number of hidden neurons within the network was also contemplated. Guided by these considerations, a variety of training algorithms and different quantities of hidden neurons were chosen and subjected to experimentation. The aim was to identify the optimal training algorithm and the optimal number of hidden neurons that collaboratively yield the most accurate and efficient network configuration. However, this selection is based on the assessment of  $r^2$  and MSE values. For the analysis of the Artificial Neural Network, MATLAB R2022a was employed. The data was initially saved in a specific folder within MATLAB before being normalized via conversion into a numeric matrix. This

process automatically established the dataset range, and the import selection was employed to import the data into the MATLAB environment. The Levenberg-Marquardt Back Propagation training algorithm, known as the improved second-order gradient method, has been identified as the optimal learning rule and subsequently applied in formulating the network structure. Specifically, the Levenberg-Marquardt Back Propagation training algorithm, configured with 38 hidden neurons, was engaged to train a network composed of one (1) output processing element and three (3) input processing elements (PEs). The chosen quantity of hidden neurons was set at 12 neurons per layer, and the performance of the network was monitored through coefficients of determination ( $r^2$ ) and Mean Squared Error (MSE). Within the network architecture, the input layer employed the hyperbolic tangent (tan-sigmoid) transfer function for calculating the layer output from input data, while the output layer utilized the linear (purelin) transfer function. The process of network generation involved partitioning the input data into training, validation, and testing sets. In this investigation, 70% of the data was allocated for network training, 15% for validation, and the remaining 15% for testing. The evaluation of the network's performance

extended over a maximum of 1000 training epochs. The network was trained with the "trainlm" function, which adjusts weight and bias parameters via Levenberg-Marquardt optimization. This function is acknowledged as one of the quickest back propagation algorithms are often regarded as the preferred supervised algorithm in the toolbox. Yes, it does however, need

additional memory compared to other algorithms. By implementing these parameters and configurations, an optimal neural network structure was established and visually represented in Fig. 1g. This identical network architecture was utilized to predict shock resistance as a singular response variable, with three input variables being employed.

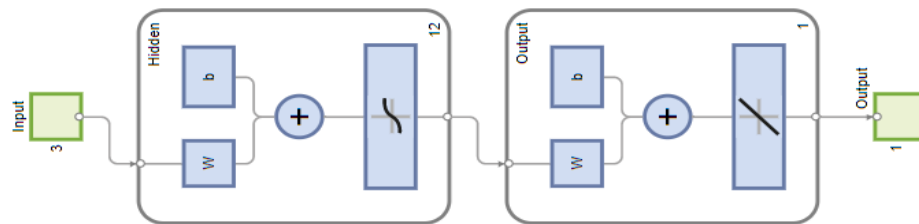


Fig. 1g: Artificial neural network architecture

The Artificial Neural Network architecture is 3-12-1, the network diagram generated for the prediction of shock resistance using the

back propagation neural network is presented in Fig. 1h

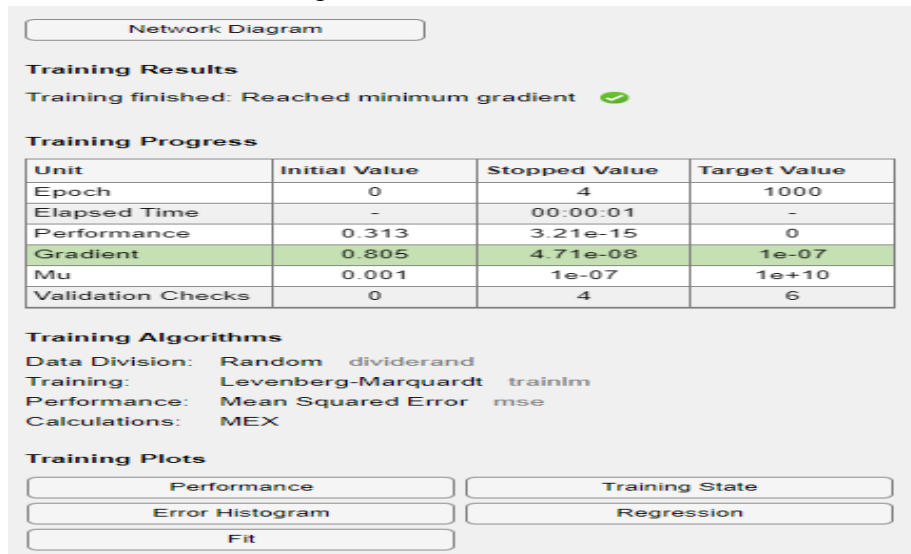
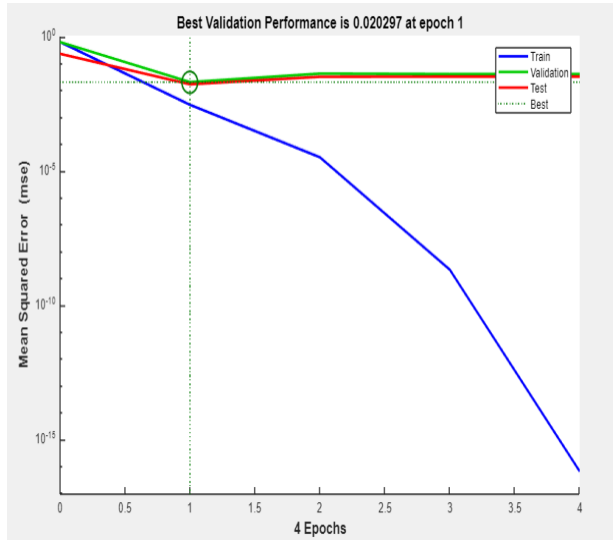


Fig. 1h: Model summary for predicting shock resistance

The network performance was determined to be 0.313 using the network training diagram

of Figure 9. Out of six (6) validation checks, four (4) were recorded. This outcome was

anticipated, as the normalization of raw data effectively addressed the issue of weight bias. Fig. 1i displays a performance evaluation plot that depicts the development of training, validation, and testing. The network's effectiveness during each of these stages is shown visually in this plot. The



**Figure 1i:** SR Performance curve of trained network predicting SR

Back propagation serves as a fundamental technique utilized in artificial neural networks for computing the contribution of error from each neuron subsequent to a batch of data training. Technically, the neural network undertakes the computation of the gradient of the loss function, thereby elucidating the error contributions originating from the chosen neurons. A lower error signifies better performance. The computed gradient value of 00000000003809, as observed in Fig. 1j, indicates the minute nature of error contributions associated with the selected neurons. In the realm of training the neural network, momentum gain (Mu) operates as a

training state is shown in Fig. 1j, which provides details on important variables like the gradient function, training gain (Mu), and validation tests. The training process and its connected aspects are clearly understood thanks to this thorough representation.

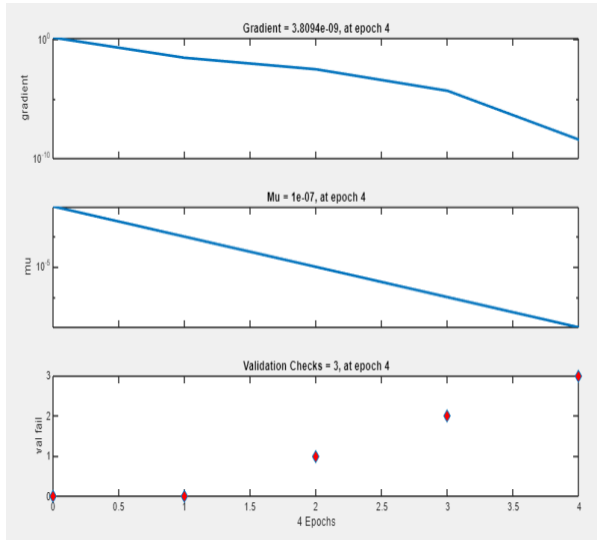


**Figure 1j:** Neural network training state for SR

control parameter for the algorithm's functionality. It characterizes the training gains, and its value is imperative to remain below unity. Notably, momentum gains of 0.0000001 underscore a network that exhibits elevated potential in predicting shock resistance (SR). Fig. 1k showcases the regression plot, illustrating the interrelation between the input variables (current, voltage, and gas flow rate) and the designated target variable (shock resistance). This image is accompanied with a visual representation of the neural network's training, validation, and testing progress, providing a complete picture of the network's performance.

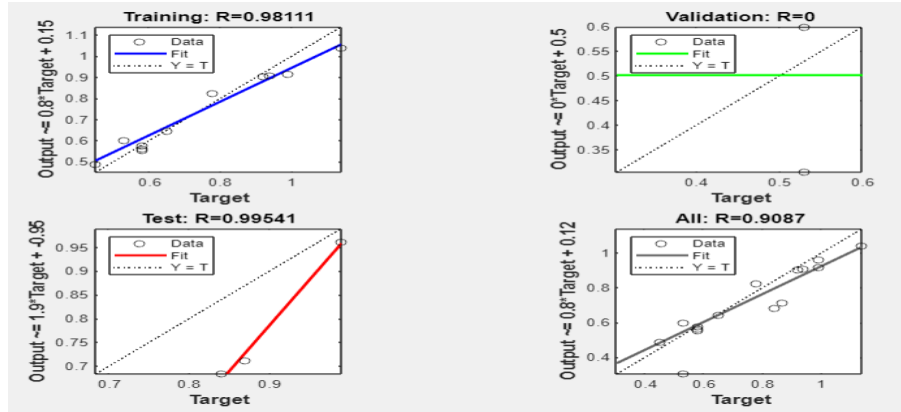


**Figure 1k:** Regression plot showing the progress of training, validation and testing

It was determined that the network had been correctly trained and could be used to predict shock resistance based on the estimated values of the correlation coefficient (R) as seen in Fig. 1k.

### 3.3 Discussion

This research employed two distinct methodologies, namely the Response Surface Methodology and the artificial neural network approach, to effectively model and forecast shock resistance as a critical factor contributing to the enhancement of Structural Integrity in Pipeline Weldment. The connection between the input parameters and the resultant responses was found to possess a quadratic nature. The findings of the sequential sum of square test, which repeatedly indicated the quadratic model as the best option due to its noticeably low p-value of 0.0001, confirmed this claim. Evaluation of the model summary statistics for all the responses unveiled  $R^2$  values hovering around 90%. This substantial  $R^2$  value underscores the robustness of the models in capturing and explaining the variations in the responses. The models also demonstrated a non-

significant lack of fit, as shown by a p-value of 0.005. These findings collectively underscore the efficacy and reliability of the developed models. The consistently high  $R^2$  values of  $> 0.9$  across all models further highlight the remarkable predictive capacity of the models. This exceptional  $R^2$  value accentuates the strength of the models in accurately forecasting the response values based on the chosen input variables. Notably, the achieved results also demonstrated that the variance inflation factor (VIF) remained at the anticipated level of 1.00, affirming the validity of the model. Design professionals decided that this alternative, which has a desirability rating of 0.918, was the best. The research demonstrates that when welding mild steel plates with tungsten inert gas, though artificial neural networks precisely predict the aforementioned reactions, the response surface methodology predicted better results.

## 4. CONCLUSION

The durability and operational lifespan of an engineered structure heavily rely on its capacity to withstand shock forces. Within the scope of this study, we have embarked

on the development of numerical models utilizing both the artificial neural network (ANN) and Response Surface Methodology (RSM) methods. The primary goal was to optimize and predict shock resistance, a critical factor, by incorporating input variables such as current, voltage, and gas flow rate. To structure our experimental approach, we harnessed the central composite design, facilitated by design expert software (version 13.0). Through the application of RSM analysis, we successfully identified optimal solutions. These solutions were determined to involve a gas flow rate of 14.667 liters per minute, a voltage of 21.280 volts, and a current of 160.000 amps. This combination led to the creation of a welded joint characterized by a shock resistance of 0.729. A strong desirability rating of 0.918 was attached to this accomplishment, highlighting the brilliance of the results attained. Additionally, we engaged an artificial neural network model in predicting the output parameters, which were subsequently compared with the predictions of the RSM methodology. Following meticulous analysis, we made a significant observation: the response surface methodology proved to be the most effective forecasting model, triumphing over the artificial neural network. This determination was grounded in the fact that RSM exhibited a higher coefficient of determination, solidifying its efficacy in this context.

## References

Baduge, SK., Thilakarathna, S, Perera, JS, Arashpour, M, Sharafi, P, Teodosio, B, Shringi, A, Mendis, P, (2022).

Artificial intelligence and smart vision for building and construction 4.0: Machine and deep learning methods and applications. *Automation in Construction*, 141, p.104440.

<https://doi.org/10.1016/j.autcon.2022.104440>

Biezma MV, Andrés MA, Agudo D, Briz E., (2020). ‘Most fatal oil & gas pipeline accidents through history: A lessons learned approach.’ *Engineering failure analysis*, 110, 104446. <https://doi.org/10.1016/j.engfailanal.2020.104446>.

Callister Jr, WD and Rethwisch DG, (2018). *Materials Science and Engineering: An introduction*. 10<sup>th</sup> Edition. ISBN: 978-1-119-40549-8.

Dogra V., (2018). Application of Welding Process Parameters Using AI Algorithm. *Turkish Journal of Computer and Mathematics Education (TURCOMAT)*, 9(2). <https://doi.org/10.17762/turcomat.v9i2.13866>.

Elahibakhsh, Y., (2023). Study of Stress and Dynamic Response of the Pipe Systems in Petrochemical Industry (Doctoral dissertation, Lamar University-Beaumont). <https://hdl.handle.net/20.500.14154/68980>.

Laska A and Szkodo M., (2020). Manufacturing parameters, materials, and welds properties of butt friction stir welded joints—overview. *Materials*, 13(21), 4940. <https://doi.org/10.3390/ma13214940>.

Li, J., (2021). Investigation and computation of the interface dynamic during magnetic pulse welding (Doctoral dissertation, Compiègne).



- Makarjian, K and Santhanam S., (2020). Micromechanical modeling of thermo-mechanical properties of high-volume fraction particle-reinforced refractory composites using 3D Finite Element analysis. *Ceramics International*, 46(4), 4381-4393. <https://doi.org/10.1016/j.ceramint.2019.10.162>
- Nwankwo C., (2021). A new smart process for pipeline integrity monitoring. <https://hdl.handle.net/2086/21013>.
- Prabowo AR, Tuswan T, Ridwan R., (2021). 'Advanced development of sensors' roles in maritime-based industry and research: From field monitoring to high-risk phenomenon measurement.' *Applied Sciences*, 11(9), 3954. <https://doi.org/10.3390/app11093954>.
- Quazi, MM, Ishak, M, Fazal, MA, Arslan, A., Rubaiee, S., Aiman, M.H., Qaban, A., Yusof, F., Sultan, T., Ali, M.M. and Manladan, S.M., (2021). A comprehensive assessment of laser welding of biomedical devices and implant materials: Recent research, development and applications. *Critical Reviews in Solid State and Materials Sciences*, 46(2), pp.109-151. <https://doi.org/10.1080/10408436.2019.1708701>.
- Rubino F, Nistico A, Tucci F, Carlone P., (2020). Marine application of fiber reinforced composites: A review. *Journal of Marine Science and Engineering*, 8(1), 26. <https://doi.org/10.3390/jmse8010026>.
- Seyyedattar M, Zendejboudi S, Butt S., (2020). 'Technical and Non-technical Challenges of Development of Offshore Petroleum Reservoirs: Characterization and Production.' *Nat Resour Res*, 29, 2147–2189. <https://doi.org/10.1007/s11053-019-09549-7>.
- Sharma A, Mukhopadhyay T, Rangappa, SM, Siengchin, S, Kushvaha V., (2022). Advances in computational intelligence of polymer composite materials: machine learning assisted modeling, analysis and design. *Archives of Computational Methods in Engineering*, 29(5), 3341-3385. <http://dx.doi.org/10.1007/s11831-021-09700-9>.
- Shojaei B, Najafi M, Yazdanbakhsh A, Abtahi M, Zhang, C., (2021). 'A review on the applications of polyurea in the construction industry.' *Polymers for Advanced Technologies*, 32(8), 2797-2812. <https://doi.org/10.1002/pat.5277>.
- Tabatabaeian A, Ghasemi AR, Shokrieh MM, Marzbanrad B, Baraheni M, Fotouhi M., (2022). 'Residual stress in engineering materials: a review.' *Advanced Engineering Materials*, 24(3), 2100786. <https://doi.org/10.1002/adem.202100786>.
- Wang X, He C, Yue Z, Li X, Yu R, Ji H, Zhao Z, Zhang Q, Lu TJ., (2022). 'Shock resistance of elastomer-strengthened metallic corrugated core sandwich panels.' *Composites Part B: Engineering*, 237, p.109840. <https://doi.org/10.1016/j.compositesb.2022.109840>.